On-Orbit Performance of Autonomous Star Trackers*

V. Airapetian, J. Sedlak, and J. Hashmall
Computer Sciences Corporation
Lanham-Seabrook, Maryland, USA 20706

Abstract

This paper presents the results of a performance study of the autonomous star trackers (ASTs) on the IMAGE and the EO-1 spacecraft. IMAGE is a spinning spacecraft without gyros or redundant precision attitude sensors, so the statistical properties of the AST are estimated simply by comparing the output observed quaternions with a rigid rotator model with constant angular momentum. The initial conditions are determined by a least-squares fit to minimize the AST residuals. An additional fit is used to remove the remaining systematic error and to obtain the inherent sensor noise. Gyro rate data are available for the EO-1 mission, so the AST noise statistics are obtained from the residuals after solving for an epoch attitude and gyro bias also using a least-squares method.

INTRODUCTION

Current and future missions need continuous and accurate three-axis attitude knowledge onboard to achieve better pointing and stability. Recently autonomous star trackers (AST) have been used onboard a number of spin-axis and three-axis stabilized spacecraft such as the New Millennium Program Deep Space-1 (DS-1), the Imager for Magnetopause-to-Aurora Global Exploration (IMAGE), and the Earth Observing-1 (EO-1) missions. The Lockheed Martin ATC AST-201R Autonomous Star Tracker (AST) is used as a primary sensor for attitude determination for these three missions. IMAGE and DS-1 are spin-stabilized spacecraft, and EO-1 is a three-axis stabilized spacecraft. Because autonomous star trackers represent a relatively new type of sensor for attitude determination and may be used in future missions such as SIRTF and MAP, it is useful to examine the statistical parameters reflecting their performance.

The AST is a "starfield-in, attitude-out" Charge Coupled Device (CCD)-based sensor. It outputs an attitude without requiring any a priori attitude knowledge. An AST-based attitude determination system can be viable without use of a digital Sun sensor (as on the EO-1 spacecraft) and even is able to perform in case of a gyro failure.

This paper presents a study of AST performance. It focuses on sensor noise statistics from the IMAGE and EO-1 missions. Some reported characteristics for DS-1 are included for comparison, but no independent DS-1 analysis was done for this paper. The IMAGE spacecraft does not carry gyros for inertial reference or other attitude sensors with enough accuracy to provide redundant

* This work was supported by the National Aeronautics and Space Administration (NASA) / Goddard Space Flight Center (GSFC), Greenbelt, MD, Contract GS-35F-4381G, Task Order no. S-43411-G.

NASA/GSFC, Guidance, Navigation and Control Center, *Flight Mechanics Symposium*, Greenbelt, MD USA, June 2001.

information for determining the AST accuracy directly, while rate data are provided from gyros on the EO-1 mission. The purpose of this paper is to determine errors in the autonomously derived attitude from the AST sensor based on multiple star measurements from analysis of IMAGE and EO-1 attitude data. The DS-1 spacecraft also carries an AST for attitude determination and, according to a recent report, performed very well during the first year of operation. It achieved accuracy (sensor noise) of about 2 arcsec in pitch and yaw and 40 arcsec in roll about the AST's optical axis (Ref. 1).

AST PERFORMANCE ON IMAGE SPACECRAFT

The IMAGE mission was launched at 20:34:43.929 UTC on March 25, 2000 from Vandenberg Air Force Base, California, aboard a Boeing Delta II 7326 launch vehicle. The IMAGE spacecraft is spin-stabilized about its Z-axis, with closed loop spin-rate control. It is an octagon-shaped spacecraft with 2.25 m diameter and 1.52 m height. Four thin wire antennas positioned 90 deg apart define the spacecraft X-Y plane. In a fully deployed configuration, the radial antennas are 250 m long. That makes the spacecraft's inertia tensor nearly diagonal.

The IMAGE attitude hardware consists of one Lockheed Martin AST, one Adcole Sun sensor, one three-axis magnetometer, a magnetic torque rod, and a nutation damper. The AST serves as the main attitude sensor providing a quaternion representing the three-axis orientation relative to the J2000 geocentric inertial frame (GCI) and angular rotation rates about each of its axes. The AST has maximum accuracy at spin rates up to 0.6 revolutions per minute (rpm). If the spin rate exceeds 1 rpm, then the star tracker is expected to lose track of stars.

The AST-to-body transformation matrix (the nominal alignment matrix) is given as (Ref. 2):

$$N_{AST-to-body} = \begin{bmatrix} 0.386710 & -0.908103 & -0.160635 \\ -0.922202 & -0.380781 & -0.067459 \\ 0.000094 & 0.174225 & -0.984706 \end{bmatrix} \tag{1}$$

Flight data from July 21, 2000 were obtained from the IMAGE website (Ref. 3) for this study. This is a time after the deployment of the radial antennas. The data file provides time and the corresponding four components of the quaternion in the sensor frame. To evaluate the performance of the AST, the observed quaternions are compared with a model. The standard deviation of the quaternion residuals is a measure of the sensor noise.

The observed AST quaternions were provided in the sensor frame. They are rotated into the body frame using the nominal alignment and an additional misalignment needed to improve the fit. The quaternions can be converted into a direction cosine matrix, $A(q)$, and then rotated so that

$$A(q_{obs}^{body}) = N_{AST-to-body} M_{123}(\varphi,\theta,\psi) A(q_{obs}^{AST}) \tag{2}$$

where the misalignment matrix, M, is expressed as a function of φ,θ,ψ, the three Euler angles for a 1-2-3 sequence.

To calculate the modeled quaternions, we assume a simple model of an axial-symmetric spinning spacecraft as described, e.g., in Ref. (4). The use of this model can be justified by the fact that in the fully deployed phase of flight, IMAGE's X- and Y-components of the moment of inertia are nearly equal to each other (within ~ 7 percent). Then, assuming torque-free rotation about the body Z-axis, the body frame attitude can be expressed analytically from the kinematic equations of motion:

$$q_{\mathrm{mod}}(t) = \begin{bmatrix} q_4' & q_3' & -q_2' & q_1' \\ -q_3' & q_4' & q_1' & q_2' \\ q_2' & -q_1' & q_4' & q_3' \\ -q_1' & -q_2' & -q_3' & q_4' \end{bmatrix} q_0 = q_0 q', \tag{3}$$

where

$$\begin{aligned} q_1' &= u_1 \cos\alpha \sin\beta + u_2 \sin\alpha \sin\beta \\ q_2' &= u_2 \cos\alpha \sin\beta - u_1 \sin\alpha \sin\beta \\ q_3' &= u_3 \cos\alpha \sin\beta + \sin\alpha \cos\beta \\ q_4' &= \cos\alpha \cos\beta - u_3 \sin\alpha \sin\beta \end{aligned}$$

$$\begin{aligned} \alpha &\equiv 0.5\,\omega_p t \\ \beta &\equiv 0.5\,\omega_l t \\ u &\equiv L_0 / |L_0| = [u_1, \quad u_2, \quad u_3]^T \\ L_0 &\equiv [L_{01}, \quad L_{02}, \quad L_{03}]^T \end{aligned}$$

In this solution, all the constants of the motion are expressed in terms of the initial values of the quaternions and L_0, the angular momentum vector in body principal coordinates.

In these equations, ω_p is the body nutation rate and is given as

$$\omega_p \equiv (1 - I_3 / I_T)\omega_3,$$

where ω_3 is the axial angular velocity of the spacecraft, I_3 is the axial moment of inertia, and I_T is the transverse moment of inertia. For the case of an axially symmetric spacecraft, I_T is equal to the X- and Y-components of moment of inertia. Moments of inertia for the IMAGE spacecraft (Ref. 2) are

$$\begin{aligned} I_x &= 14710.5\ \mathrm{kg\text{-}m^2}, \\ I_y &= 14688.8\ \mathrm{kg\text{-}m^2}, \\ I_z &= 29041.9\ \mathrm{kg\text{-}m^2}. \end{aligned}$$

Because the values of I_x and I_y are close, it is valid to approximate $I_x = I_y = I_T$ and equal to 14700 kg-m^2.

Also, ω_l is the inertial nutation rate, which can be expressed in terms of the body nutation rate as

$$\omega_l = \frac{I_3}{(I_T - I_3)\cos\theta}\omega_p$$

where $\cos\theta = L_3 / L$, and L_{01}, L_{02}, L_{03} are the X-, Y- and Z-components of the angular momentum vector, and L is its absolute value.

The residuals, dq, between the observed, q_{obs}^{body}, and modeled, q_{mod}, quaternions are

$$dq = (q_{obs}^{body})^* q_{\mathrm{mod}}, \tag{4}$$

where $(q_{obs}^{body})^*$ is the conjugate of the observed quaternion rotated into the body frame. A loss function, F, is constructed from the squares of the vector parts of the quaternion residuals:

$$F = \frac{1}{n}\sum_{i=1}^{n} d\vec{q}(t_i)\cdot d\vec{q}(t_i) \tag{5}$$

where n is the total number of data points.

We then solve for 6 independent parameters: 3 components of the quaternion and the components of the angular momentum vector, so as to minimize the loss function specified in Eq. (5). The MATLAB subroutine ***fminsearch*** was used to find the set of parameters minimizing the loss function. Initial guesses for the x and y components of the angular velocity were taken to be zero, while the initial axial component of the angular velocity was derived directly from the periodicity of the observed quaternions.

The resulting quaternion residuals are very small for the z-axis but were found to have mean value of roughly 0.2 deg on the X- and Y-axes. Note that the negative Z-axis is only 10 deg from the AST boresight. Thus, the minimization finds the rotation phase angle but is less successful with the spin direction. This indicates there may be a misalignment between the AST-attitude (after rotation to the body frame using nominal alignment) and the principal rotation axis. This may be due to a combination of sensor misalignment and an offset of the principal axis from the body Z-axis causing some coning.

The variance in the attitude residuals is caused by the true sensor noise plus model errors. Besides the sensor misalignment, there may be a deviation from uniform rotation due to environmental perturbations or the non-symmetry of the transverse axes. Therefore, the standard deviation of the residuals represents only an upper bound for the AST error.

The mean residuals can be used as a starting point for a search for a misalignment matrix. The best misalignment found has the Euler angles $\varphi = 0.2032$ deg and $\theta = -0.1050$ deg. The ψ rotation is kept at zero since it corresponds to an unobservable phase (absorbed by the value of the epoch quaternion found by the minimization).

After correcting for the misalignment, the mean attitude residuals are greatly reduced. The X-, Y- and Z-axis residuals from the vector part of the dq in Eq. (4) are shown in Fig. 1. The standard deviation on the X-axis (the transverse axis with the least systematic error) is 61 arcsec. For the Y- and Z-axes, the standard deviations are 67 and 80 arcsec, respectively. Because the AST boresight lies mostly in the X-Z plane of the spacecraft body system, the body Y-axis will be the least sensitive to the rotation errors.

It is clear from Fig. 1 that some systematic error remains in the residuals and that various "oscillation" frequencies are present in X-, Y- and Z-components of the quaternion residuals. To account for them, we have selected ten of the local maxima and applied a parabolic fit to each. By subtracting the parabola, the remaining residual errors are "flattened" and the inherent sensor noise can be determined by calculating the standard deviation.

The time span around each peak used for the parabolic fit was varied to be sure of the robustness of the noise estimate. Time spans ranging from 5 sec to 160 sec were tried. The means of the standard deviations from all ten peaks are shown in Fig. 2 as a function of the time span of the fit.

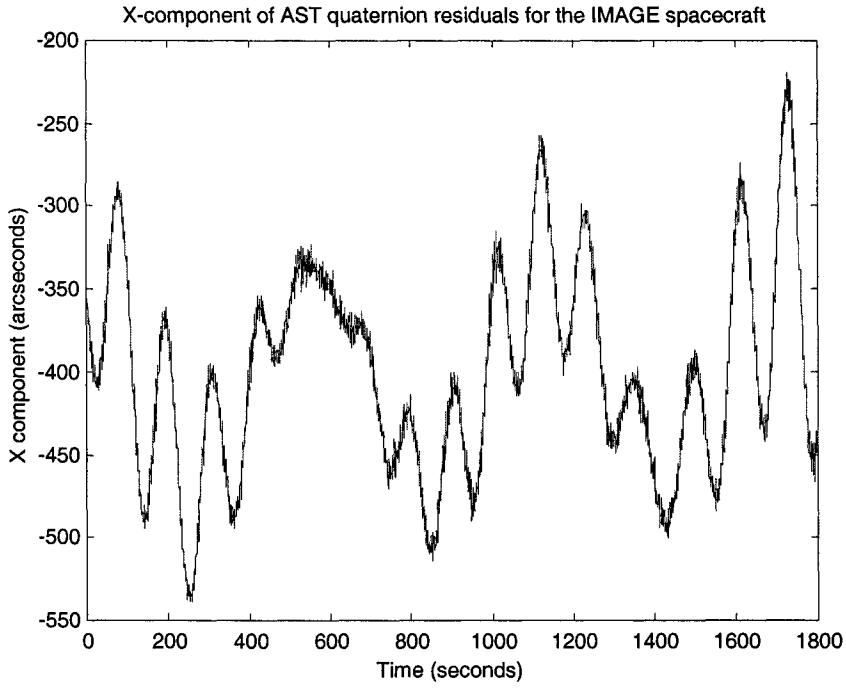

Figure 1a. Attitude residuals (X-component) comparing the AST and the torque-free rigid rotator model for the IMAGE spacecraft.

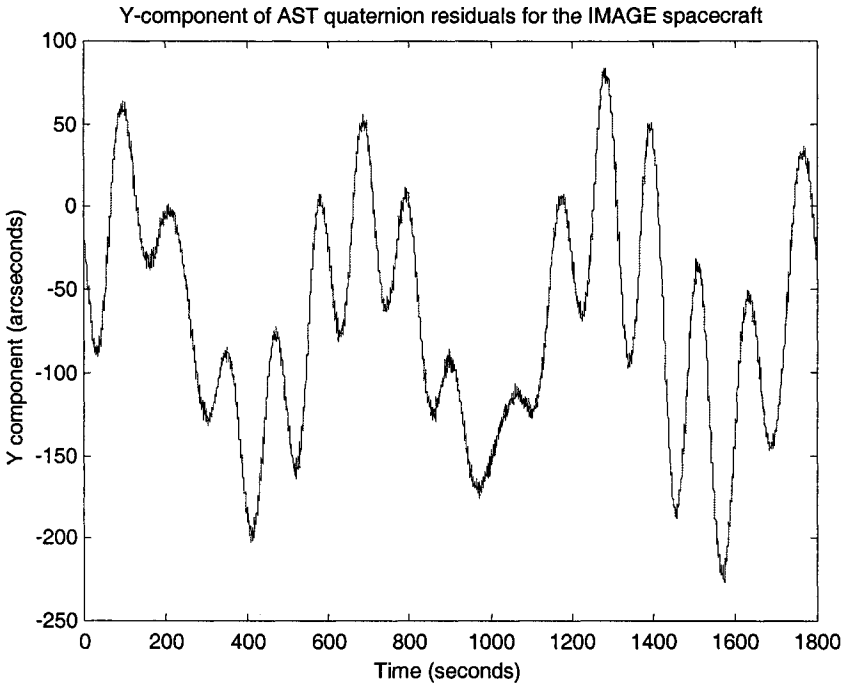

Figure 1b. Attitude residuals (Y-component) for the IMAGE spacecraft.

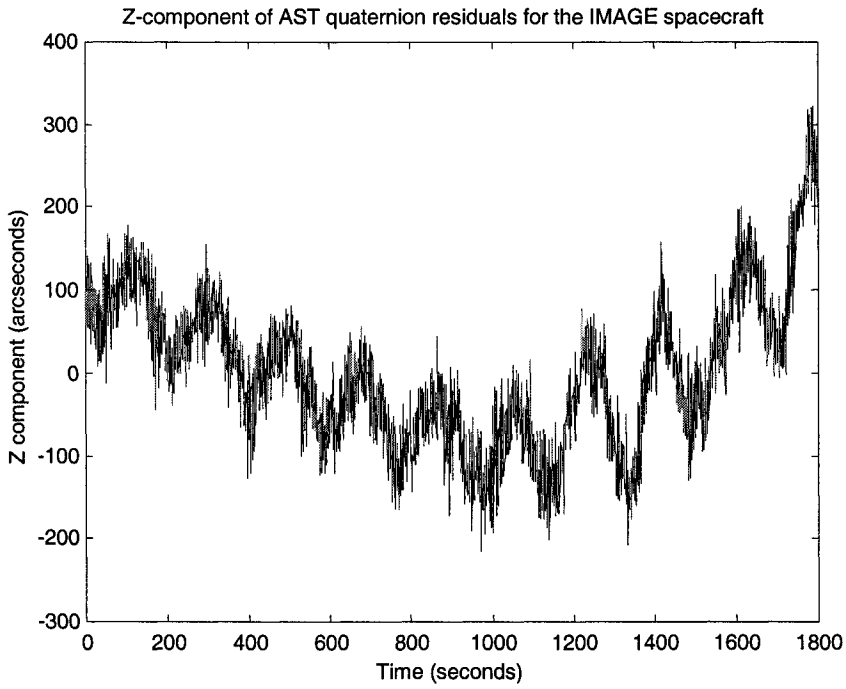

Figure 1c. Attitude residuals (Z-component) for the IMAGE spacecraft.

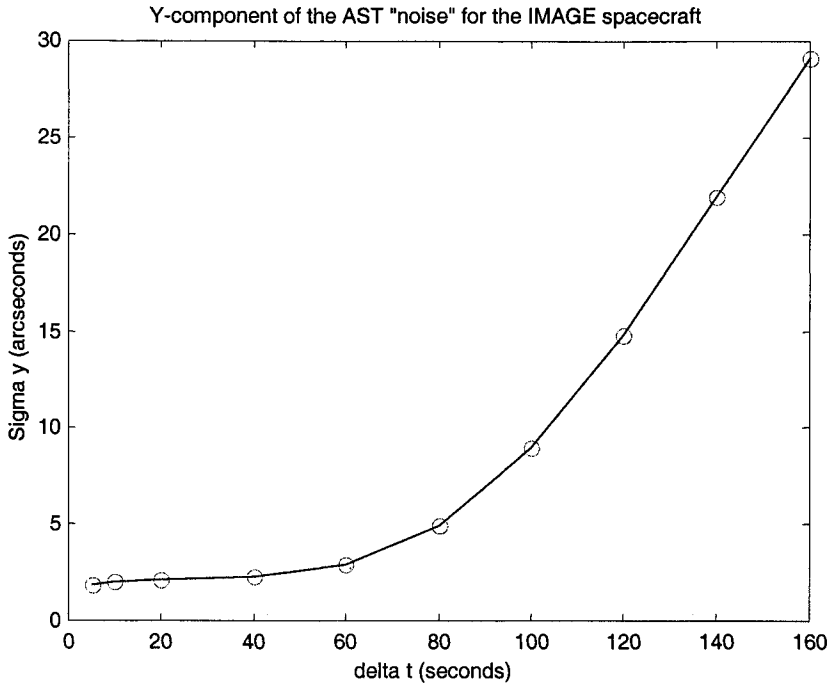

Figure 2. Y-component of the apparent AST noise averaged over ten peaks from Fig. 1 versus time span used for subtracting the systematic error.

Figure 2 reveals a characteristic plateau for parabolic fit time spans up to about one minute. The apparent sensor noise from this flat part of the graph is about 2.1 arcsec for the Y-axis. Similar analysis gives 4.7 arcsec and 22.9 arcsec for the sensor X- and Z-axes. These are our estimates of the inherent noise for the AST onboard IMAGE.

AST PERFORMANCE ON EO-1 SPACECRAFT

The EO-1 mission, managed by NASA's Goddard Space Flight Center, has three revolutionary land-imaging instruments collecting multispectral and hyperspectral scenes. EO-1 was launched on a Boeing Delta II rocket from Vandenberg Air Force Base on November 21, 2000.

The EO-1 is three-axis stabilized for nadir pointing. The pointing accuracy is 0.03 deg on all three axes and jitter is less than 5 arc-seconds. The EO-1 hardware consists of one Lockheed Martin Autonomous Star Tracker (AST 201R) which provides 3-axis attitude knowledge and gyros providing 3-axis body rates.

Analysis of the EO-1 AST performance was accomplished using attitude data (AST quaternions and gyro rates) for November 23, 2000 from 16:24:01 to 18:42:01 UT. The analysis was performed using the Matlab-based Attitude Determination System (ADS) (Ref. 5). The ADS estimates an epoch attitude and gyro bias vector from the AST and gyro input data using a batch least-squares method. This attitude is propagated using the bias-corrected gyro data to generate an attitude history.

Two intervals with nearly constant rates were selected. During such periods, the accuracy of the attitude solution is insensitive to errors in gyro calibration since gyro biases are included in the state vector. Such solutions were found and used as "truth" in determining the AST performance.

To determine the sensor performance, the attitude solutions were compared to the AST observations, and statistics on their differences (sensor residuals) were accumulated. The mean residuals are zero, as expected, because the AST is the only sensor used. The plots of the AST residuals expressed in the sensor frame are presented in the Fig. 3.

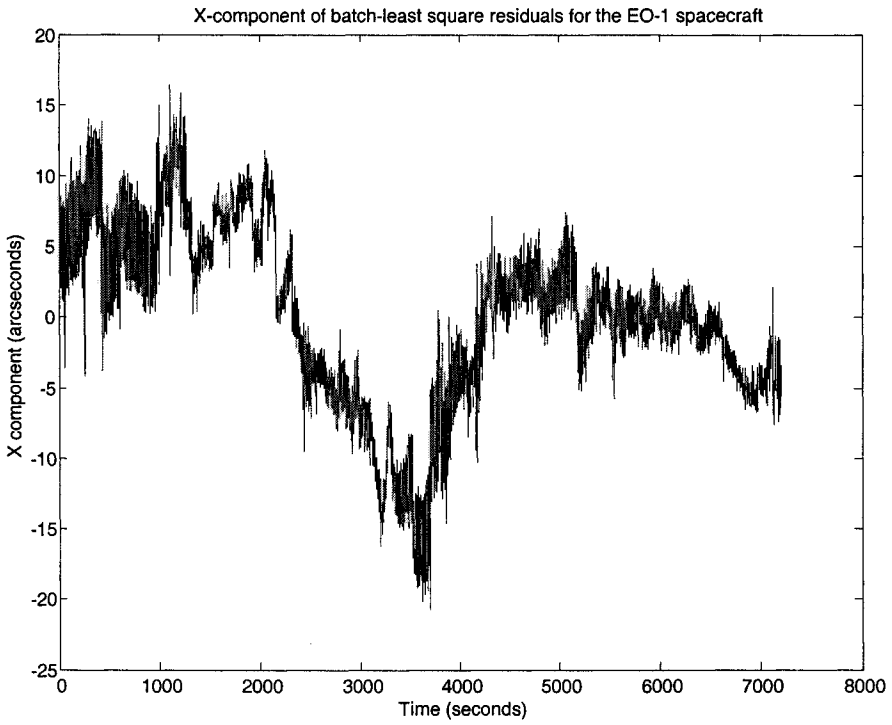

Figure 3a. Attitude residuals (X-component in the sensor frame) comparing AST and ground attitude solution for EO-1.

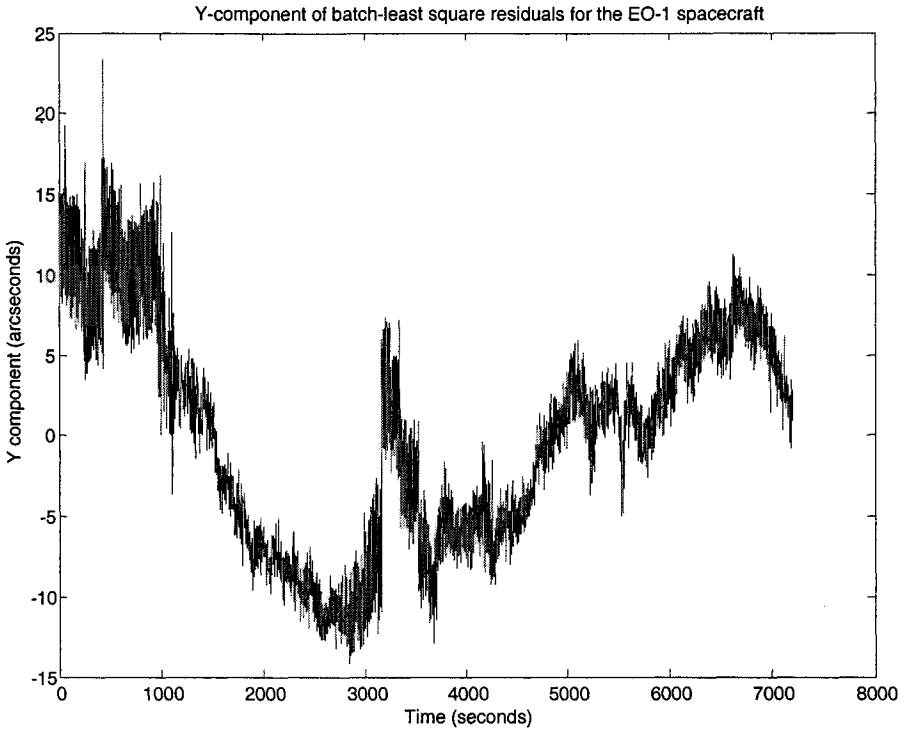

Figure 3b. Attitude residuals (Y-component in the sensor frame) for EO-1.

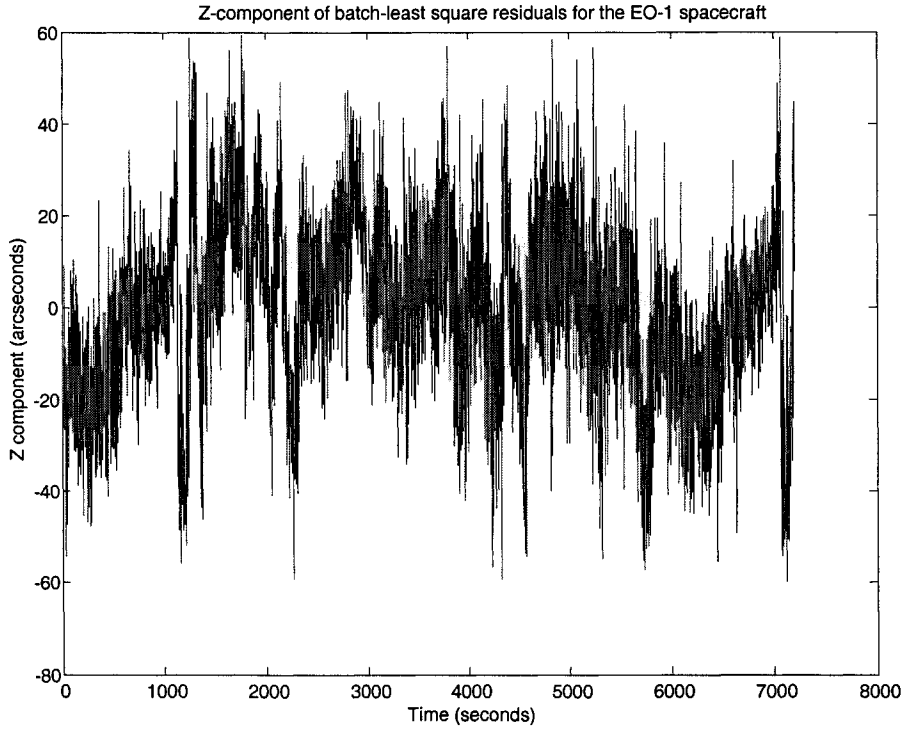

Figure 3c. Attitude residuals (Z-component in the sensor frame) for EO-1.

Low-frequency variations present in the residuals indicate systematic errors on time-scales of hundreds of seconds. These possibly are accounted for by variations in the stars crossing the sensor field of view at any given time. The number of stars, their magnitudes, and the distribution across the field of view all might affect the attitude estimate. The actual inherent AST sensor noise is probably better represented by the standard deviations of the higher frequency variations seen in Fig. 3.

The standard deviations of the AST residuals for the entire 2-hour EO-1 data set are 6.2, 6.9, and 18.1 arcsec for the X-, Y-, and Z-components, respectively. The root-sum-square of the transverse X- and Y-components is 2–3 times larger than found for the ASTs on IMAGE and DS-1, as discussed above. An improved estimate of the inherent AST noise can be found by first removing the effects of the systematic errors; however, it should be emphasized that actual spacecraft control is likely to depend on the total error and not just on this somewhat subjectively determined inherent error.

To estimate the inherent AST noise, a number, N, of relatively flat intervals were selected for each AST component (7 for X, 5 for Y, and 6 for Z). The mean residual was subtracted from each interval and the variances were computed. With the mean values removed, the total variance is

$$\text{var} = \frac{\sum_{i=1}^{N} N_i \, \text{var}(i)}{\sum_{i=1}^{n} N_i}, \tag{6}$$

where N_i is the number of observations and var(i) is the variance for the i-th interval. The square root of the total variance is our estimate of the inherent AST noise. Figure 4 shows a sample of typical "flat" intervals for each of the components. The selected intervals cover roughly 50 percent of the entire 2-hour data set for the X- and Y-axes and 30 percent for the Z-axis. The actual time spans range from 500 to 1000 sec. The noise standard deviations range from 1.0 to 2.6 arcsec for the transverse components and from 8.5 to 13.8 arcsec for the Z-axis. The total errors from Eq. (6) are found to be 1.7, 1.7, and 11.6 arcsec for the X-, Y-, and Z-components, respectively. These errors are consistent with the AST performance found for IMAGE and reported for DS-1.

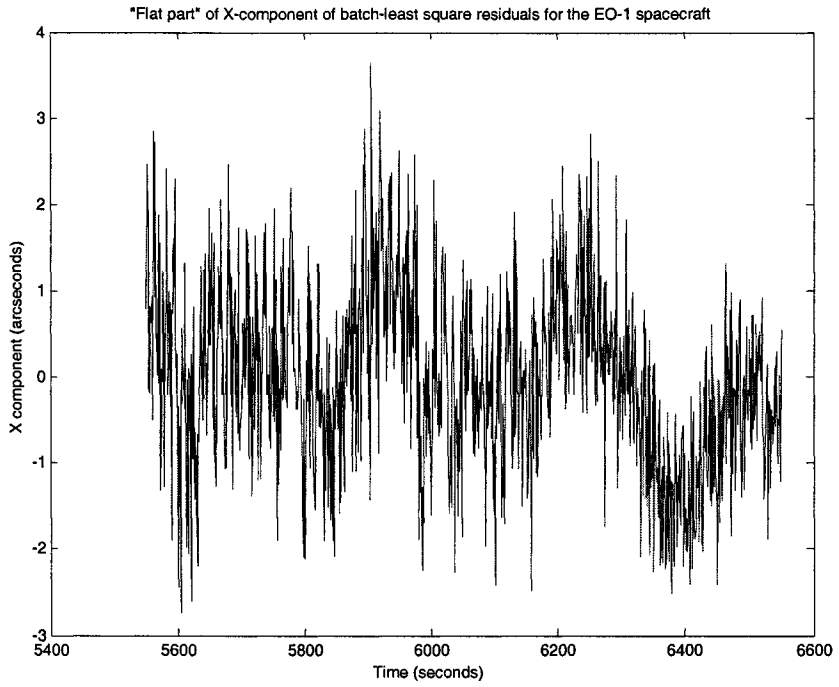

Figure 4a. Attitude residuals (X-component in the sensor frame) comparing AST and ground attitude solution for EO-1 showing a selected interval where the AST residuals are relatively flat.

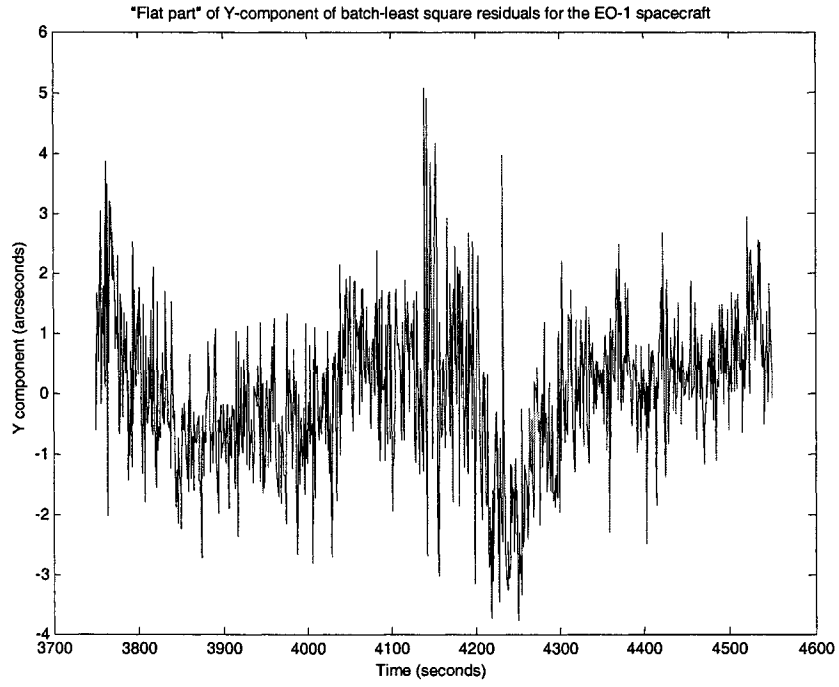

Figure 4b. Attitude residuals (Y-component in the sensor frame) for EO-1 showing a selected interval where the AST residuals are relatively flat.

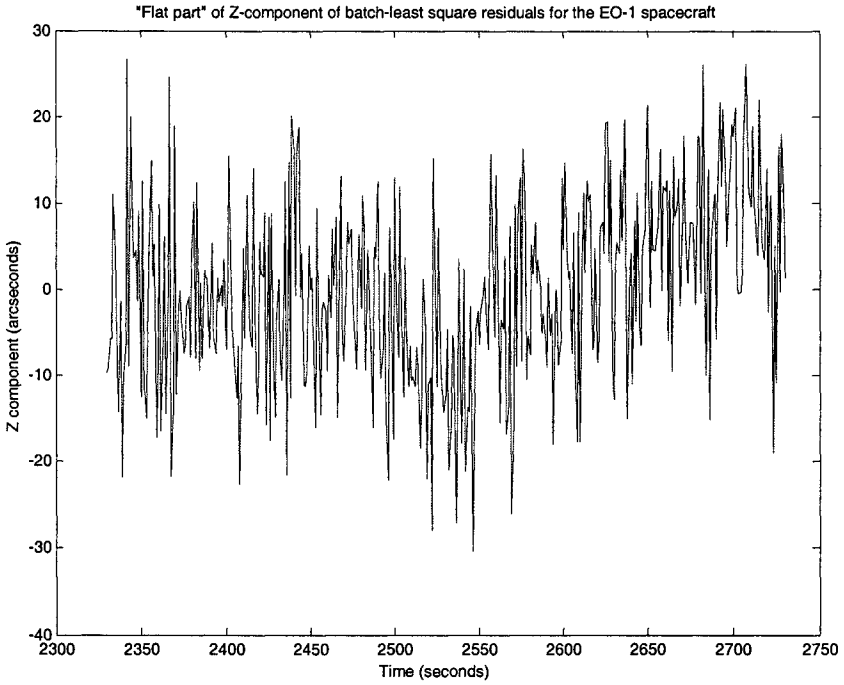

Figure 4c. Attitude residuals (Z-component in the sensor frame) for EO-1 showing a selected interval where the AST residuals are relatively flat.

CONCLUSIONS

In this study we have used in-flight data from the IMAGE and EO-1 missions to estimate the uncertainty of the AST. The noise of the AST onboard IMAGE has been estimated by comparing quaternions from the AST with reference quaternions calculated with a torque-free model for an axial-symmetric spacecraft. The initial quaternion and angular momentum are determined by minimizing a loss function as a function of these six solve-for parameters. A misalignment matrix was estimated to improve the match between observed and modeled attitudes. The remaining systematic errors were removed by fitting and subtracting parabolas from selected subsets of the data. For EO-1, both AST quaternions and gyro rate data are available. The AST noise statistics were obtained from the AST residuals after solving for an epoch attitude and gyro bias. Again, it was necessary to remove systematic errors by processing selected subsets of the data.

A summary of estimated noise parameters for ASTs onboard the IMAGE, EO-1, and DS-1 spacecraft is given in Tables 1 and 2. Table 1 shows the AST noise as determined from residual statistics over moderately long time periods (30 min for IMAGE and 140 min for EO-1). Table 2 shows noise for selected time intervals with systematic variations removed. However, these systematics may be a real source of onboard error, as seems to be indicated by the gyro-propagated attitude solution for EO-1, or they may be due to our estimation method (in particular, the symmetric rigid rotator model for IMAGE). In either case, Table 1 shows upper bounds for the AST noise. Table 2 indicates the apparent inherent noise after the somewhat

subjective subtraction of the systematic errors. The inherent noise parameters estimated this way (and the reported noise for DS-1) are all consistent with each other.

Table 1. AST Noise Including Systematic Errors.

	IMAGE	EO-1
1-σ AST X residuals (arcsec)	61	6.2
1-σ AST Y residuals (arcsec)	67	6.9
1-σ AST Z residuals (arcsec)	88	18.1
Attitude accuracy requirement (arcsec)	360	108

Table 2. AST Noise With Systematic Errors Excluded. AST noise as reported for DS-1 [Ref. 1] is presented for comparison.

	IMAGE	EO-1	DS-1
1-σ AST X residuals (arcsec)	2.1	1.7	2
1-σ AST Y residuals (arcsec)	4.7	1.7	2
1-σ AST Z residuals (arcsec)	22.9	11.6	40

REFERENCES

1. S. S. Lisman, NASA/Jet Propulsion Laboratory, private communication, January 20, 2001

2. M. Challa, et al., *IMAGE Attitude Support Post-Launch Report*, prepared for GSFC by CSC, June 2000

3. The IMAGE homepage is at http://image.gsfc.nasa.gov/

4. J. R. Wertz (ed.), *Spacecraft Attitude Determination and Control*, D. Reidel Publishing Company, Dordrecht, The Netherlands, 1978, p. 529

5. J. Landis, et al., *Multimission Three-Axis Stabilized Spacecraft (MTASS) Flight Dynamics Support System Functional Specifications, Rev. 1*, Computer Sciences Corporation, 554-FDD-91/070R1UD0, CSC/TR-91/6071R1UD0, September 1995